

structure-factor magnitudes are obtained from experiment. Nevertheless, the extrapolation of data, in both cases, corresponds to determination of an analytic function whose squared modulus is a function of maximum entropy measure. The definition for entropy measure is that given by Ponsonby (1973),

$$H' = \int_V \ln \rho(\mathbf{r}) dV, \quad (29)$$

$V$  being the unit-cell volume. Ponsonby emphasizes that this is strictly only a measure of relative entropy of the real power spectrum of an underlying signal. In this sense maximum  $H'$  corresponds to maximum entropy measure  $\rho(\mathbf{r}) = |g(\mathbf{r})|^2$ , and a maximum-entropy distribution function for  $G_h$ , the transform of  $g(\mathbf{r})$ . Equation (6) shows that such a distribution requires a maximum determinant  $D_m$ . Moreover, Ponsonby points out that entropy maximization provides a unique, smooth autocorrelation function in exact agreement with its observed values which concedes greatest possible ignorance of its unobserved values. This corresponds to the liberty of choosing by unspecified criteria the vectors ( $\mathbf{L}' + \mathbf{h}_p$ ) which direct the formulation of  $D_m$  and allow as many different appended rows and columns in  $D_{m+1}$  as there may be reasonable choices of  $\mathbf{L}'$ .

The formalisms of the maximum entropy and maximum determinant methods have been cast in

parallel form and shown to be equivalent. With only the restrictions that (electron) density be positive, and that matrices and determinants be of small enough order to be positive definite, the two equivalent formulations yield identical results and provide an information-theoretic interpretation of the maximum determinant.

This work was supported in part by the Robert A. Welch Foundation through Grant A-742, and by the Research Corporation through a Cottrell Research Grant.

#### References

- BODEWIG, E. (1959). *Matrix Calculus*. Amsterdam: North-Holland.
- BURG, J. P. (1967). *Maximum-Entropy Spectral Analysis*. 37th Annual International SEG Meeting, October 31. Oklahoma City. Reprinted in *Modern Spectrum Analysis* (1978), edited by D. G. CHILDERS, pp. 34–41. New York: IEEE Press.
- COLLINS D. M. (1978). *Acta Cryst.* A **34**, 533–541.
- KARLE, J. & HAUPTMAN, H. (1950). *Acta Cryst.* **3**, 181–187.
- MCDONOUGH, R. N. (1974). *Geophysics*, **39**, 843–851.
- PAPOULIS, A. (1973). *IEEE Trans. Inf. Theory*, **19**, 9–12.
- PONSONBY, J. E. B. (1973). *Mon. Not. R. Astron. Soc.* **163**, 369–380.
- SAYRE, D. (1952). *Acta Cryst.* **5**, 60–65.
- SHANNON, C. E. & WEAVER, W. (1949). *The Mathematical Theory of Communication*. Univ. of Illinois Press.
- TSOUCARIS, G. (1970). *Acta Cryst.* A **26**, 492–499.

*Acta Cryst.* (1982). A **38**, 132–137

## The Layered Perovskites $(\text{C}_3\text{H}_7\text{NH}_3)_2\text{MnCl}_4$ (PAMC)\* and $(\text{C}_2\text{H}_5\text{NH}_3)_2\text{MnCl}_4$ (EAMC):† Birefringence Studies and the Symmetry of the Commensurately Modulated $\varepsilon$ Phase of PAMC

BY IAN HEDLEY BRUNSKILL AND WULF DEPMEIER

*Université de Genève, Chimie Appliquée, 30 quai Ernest Ansermet, CH 1211 Genève, Switzerland*

(Received 21 May 1981; accepted 4 August 1981)

#### Abstract

By measuring the birefringence on (001) platelets of PAMC as a function of temperature, previously determined phase transitions have been confirmed. Large effects were measured on passing through the normal–incommensurate  $\delta \rightarrow \gamma$  transition and through the normal–commensurate  $\zeta \rightarrow \varepsilon$  transition, whereas the commensurate–normal  $\varepsilon \rightarrow \delta$  and the incommen-

surate–normal  $\gamma \rightarrow \beta$  transitions are less pronounced, in accordance with former thermoanalytic studies. A comparison is made with a similar study on EAMC. The optical anisotropy is discussed for both compounds in terms of the structural changes of the perovskite-type layers. Power laws of the form  $\Delta n \sim (1 - T/T_c)^{2\beta}$  are used to describe the birefringence where appropriate. By analyzing systematic extinctions amongst main and satellite reflexions, the  $\varepsilon$  phase of PAMC is proposed to be a (3 + 1)-dimensional commensurately modulated version of the  $\delta$  phase. The superspace group is determined to be  $P_{511}^{Abma}$ . With the

\* Bis(*n*-propylammonium) tetrachloromanganate.

† Bis(ethylammonium) tetrachloromanganate.

rationality of the modulation vector this leads to the three-dimensional space group *Pbma*.

### Introduction

The compounds  $(C_nH_{2n+1}NH_3)_2MnCl_4$  may be regarded as layered perovskites, because they contain layers of corner-sharing  $MnCl_6$  octahedra which

closely resemble (100) slabs of three-dimensional perovskites. The alkylammonium cations are attached from both sides to these layers by  $N-H \cdots Cl$  hydrogen bonds. The alkyl residues point away from the layers and the so-formed neutral strata have only van der Waal's contacts between one another. The structural details have often been described (see references) and a picture of the structure may be found, for example, in Depmeier (1976).

Table 1. *Characteristics of phases and phase transitions of EAMC and PAMC*

Under  $T_c$  are listed the transition temperatures from this study, as observed on heating; absolute accuracy  $\pm 2$  K. For comparison, the column DSC lists transition temperatures (K), enthalpies ( $\text{kJ mol}^{-1}$ ) and entropies ( $\text{J mol}^{-1} \text{K}^{-1}$ ) from the thermoanalytical studies of (Depmeier, Felsche & Wildermuth, 1977).

Phase	$T_c$	DSC	Birefringence characteristics; change	Structural characteristics	References
EAMC					
$\alpha$			Uniaxial	<i>I4/mmm</i> ; no resultant tilting of octahedra layer; full disorder of $RNH_3$ groups	*
$\beta$	$T_{c1}$ : 420.0	424	Power law $\Delta n^\beta \propto (1 - T/T_{c1})^{0.61}$	<i>Abma</i> ; washboard-like tilting of octahedra layer; preferred orientation, but partial disorder of $RNH_3$ groups	(a), (b)
	$T_{c2}$ : 224.4	225 653 2.9	4.5%		
$\gamma$			Power law $\Delta n^\gamma \propto (1 - T/T_{c2})^{0.24}$	<i>Pbca</i> ; washboard-like tilting of octahedra layer, but additional <i>c</i> tilt; frozen-in $RNH_3$ groups	(c)
PAMC					
$\alpha$			Uniaxial	<i>I4/mmm</i> ; no resultant tilting of octahedra layer; full disorder of $RNH_3$ groups	*
$\beta$	$T_{c1}$ : 441.0	446	Power law $\Delta n^\beta \propto (1 - T/T_{c1})^{0.60}$	<i>Abma</i> ; like $\delta$ -PAMC	*
	$T_{c2}$ : 388.0	396 251 0.63		Slow increase of modulation amplitude of $\gamma$ -PAMC	*
$\gamma$			Linear $\Delta n \simeq -0.64 \times 10^{-3} T$	Like $\delta$ -PAMC, but incommensurately modulated, two modulation vectors $\parallel \mathbf{a}^*$ $\mathbf{q}_1^* \simeq 0.17, \mathbf{q}_2^* \simeq 0.05$	(d)
	$T_{c3}$ : 339.5	344 795 2.34	7%	Modulation amplitude goes to zero	
$\delta$			Power law $(\Delta n^\delta - \Delta n_{T_{c3}}^\delta) \propto (1 - T/T_{c3})^{0.46}$	<i>Abma</i> ; washboard-like tilting of octahedra layer; preferred orientation, but partial dynamical disorder of $RNH_3$ groups	(e), (f)
	$T_{c4}$ : 168.0	165 50 —	<1%	Slow increase of modulation amplitude of $\epsilon$ -PAMC	*
$\epsilon$			Linear $\Delta n \simeq 0.015 \times 10^{-3} T$	<i>Pbma</i> ; like $\delta$ -PAMC, but commensurately modulated, modulation vector of $1/3 \parallel \mathbf{b}^*$	
	$T_{c5}$ : 112.5	110 422 4	5%	Modulation amplitude goes to zero	
$\zeta$				<i>Pbca</i> ; washboard-like tilting of octahedra layer, but additional <i>c</i> tilt; frozen-in $RNH_3$ groups	

References: (a) Depmeier (1976); (b) Depmeier & Heger (1978); (c) Depmeier (1977); (d) Depmeier (1981); (e) Peterson & Willet (1972); (f) Depmeier & Mason (1978).

\* Not yet rigorously proven.

Re-orientations of the hydrogen-bonding system, owing to increase of order with decreasing temperature, lead to various phase transitions. The alkyl chain, now, has an additional influence as shown by the fact that the propylammonium compound has a much more complicated phase transition behaviour than the ethyl compound, these two compounds being compared in this study by means of birefringence measurements.

Table 1 lists, besides the results of this investigation, some brief information on structural characteristics of the different phases of the ethyl and propyl compounds.

One of the most peculiar properties of PAMC is the fact that it forms an incommensurately modulated phase,  $\gamma$ -PAMC, with two modulation vectors in the same direction ( $a^*$ ; Depmeier, 1981). Below that phase we find the normal  $\delta$  phase. Below the  $\delta$  phase there is another peculiar phase which up to now has always been described as a threefold superstructure (Depmeier, Felsche & Wildermuth, 1977). This paper now presents the results of an analysis of the superstructure reflexions. It turns out that they belong to a commensurately modulated version of the  $\delta$  phase, the modulation vector being perpendicular to those of the  $\gamma$  phase, *i.e.* in the  $b^*$  direction.

Birefringence measurements provide a very sensitive means of detecting phase transitions and have been successfully employed for the description of the phase sequence of the methyl compound (Knorr, Jahn & Heger, 1974). In the present paper we report on the birefringence observed in EAMC and PAMC and compare it with the results obtained from diffraction studies.

### Optical studies

#### Experimental

Crystals of EAMC and PAMC were grown by evaporating water/ethanol solutions of  $MnCl_2$  and alkylammonium chlorides. As the crystals are hygroscopic, sample preparation was performed in a glove box; cleaved (001) platelets of thickness  $\sim 70$   $\mu m$  and up to 10  $mm^2$  cross section were examined under a microscope and regions of twinning observed, commonly in the form of strips up to 1 mm wide and parallel to the tetragonal  $a$  and  $b$  axes; regions large enough for easy compensation were sought.

The birefringence was measured with a Leitz  $MgF_2$  tilting compensator in combination with a Leitz Orthoplan microscope. Low-temperature studies were made with an Oxford Instruments CF204 helium-exchange gas continuous-flow cryostat in a horizontal mode; a Zeiss heating stage 1350 with nitrogen flushing was available for temperatures above 300 K. The

relative accuracy in the temperature was  $\pm 0.1$  K, whereas that in absolute temperature was estimated as 2 K; the error in the phase difference was of the order of 3 nm. Both compounds, however, begin to decompose in the region of 410–430 K and this further limits the experimental accuracy in the vicinity of  $T_{C1}$ , the temperature of the orthorhombic ( $Abma$ )–tetragonal ( $I4/mmm$ ) phase transition.

### Results

A room-temperature study with conoscopic illumination indicates that EAMC is biaxial negative and PAMC biaxial positive. The temperature dependence of the birefringence for the two compounds is shown in Fig. 1. Apart from the  $\beta \rightarrow \gamma$  transition in PAMC at  $T_{C2}$ , the transitions are easily located. Previous thermo-analytic investigations (Depmeier, Felsche & Wildermuth, 1977) have identified the nature of the transitions and the intensities of the thermal peaks agree reasonably well with the quantities measured in the present study.

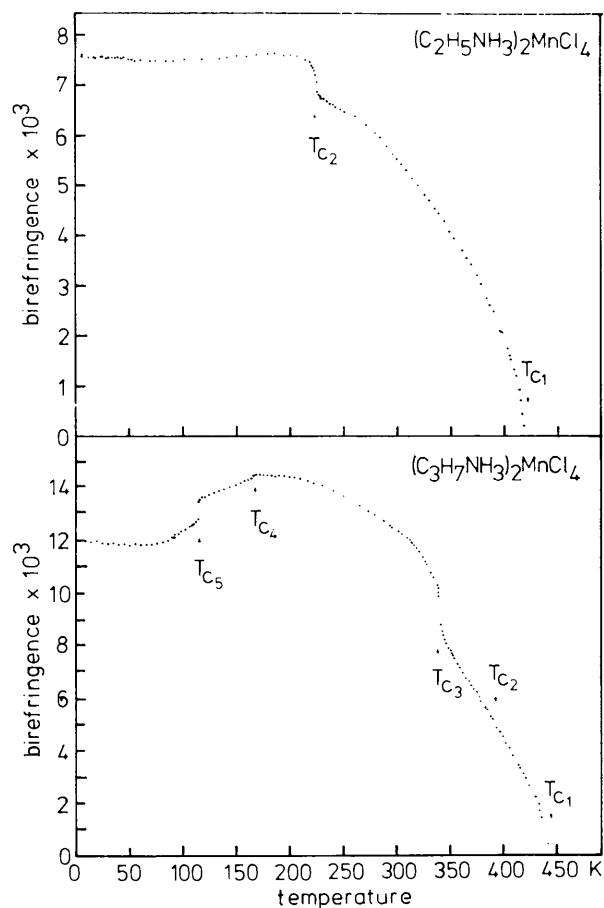


Fig. 1. The birefringence for EAMC (above) and PAMC (below). The transition temperatures are indicated and are listed in Table 1.

In EAMC the birefringence observed in the  $\beta$  phase arises from the washboard-like puckering of the  $\text{MnCl}_6$  octahedra layers, and follows a power law of the form  $(1 - T/T_c)^{2\beta}$ , where  $\beta$  is the critical exponent of the order parameter. For order-disorder transitions the birefringence is proportional to the square of the order parameter if the crystal symmetry changes at the transition (Egert, Jahn & Renz, 1971). A log-log plot between 295 and 418 K in Fig. 2 testifies to this behaviour and a least-squares analysis gives  $2\beta = 0.61 \pm 0.01$ . At  $T_{c2}$  the octahedra undergo an additional rotation about the  $c$  axis which is responsible for the rather large increase of about 4.5% in  $\Delta n$  at this temperature. A power law with  $2\beta = 0.24 \pm 0.01$  describes the birefringence  $\Delta n^\gamma(T) = \Delta n(T) - \Delta n^\beta(T_{c2})$  for the temperature range 200 to 223 K, where the superscripts indicate the phases. In contrast to the  $\alpha \rightarrow \beta$  transition, a thermal hysteresis,  $T_{c2}^{\text{heating}} - T_{c2}^{\text{cooling}}$ , of 0.4 K was observed.

The optical anisotropy in PAMC, however, displays far more variety in its temperature dependence but certain characteristics are similar. The continuous phase transition at  $T_{c1}$  is again due to the tilting of the  $\text{MnCl}_6$  octahedra and  $\Delta n^\beta(T) \sim (1 - T/T_{c1})^{0.60}$ , as indicated in a log-log plot in Fig. 2, where the linearity is destroyed at  $T_{c2}$ , at which temperature the incommensurately modulated  $\gamma$  phase appears, with the wave vector  $\mathbf{q}^* \parallel \mathbf{a}^*$  and amplitude  $A \parallel \mathbf{c}$ . The birefringence varies linearly with temperature in this region and  $\Delta n^\gamma(T) \simeq -0.064 \times 10^{-3} T$ .

As far as we know, the amplitude increases until  $T_{c3}$ , whereupon it drops to zero, giving rise to a 7% increase in  $\Delta n$ . In the  $\delta$  phase the increasing octahedra tilt is responsible for the power-law behaviour observed, with  $\Delta n^\delta(T) = \Delta n(T) - \Delta n^\gamma(T_{c3}) \sim (1 - T/T_{c3})^{0.46}$ , for  $300 \leq T \leq 338$  K. A hysteresis of 1.5 K was observed at the  $\gamma \rightarrow \delta$  transition. At  $T_{c4}$  another modulation appears with  $A \parallel \mathbf{c}$  but  $\mathbf{q}^* \parallel \mathbf{b}^*$ , which effectively causes an approximately linear decrease in the birefringence, with

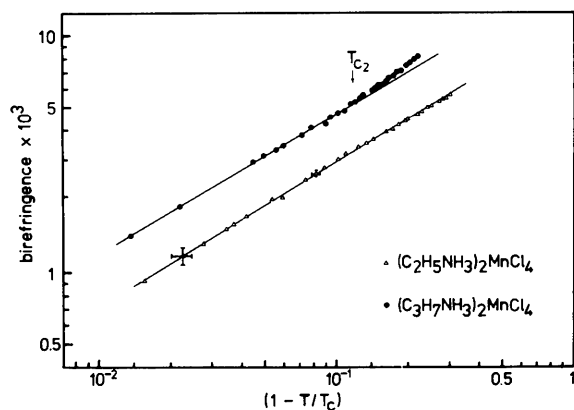


Fig. 2. The power-law behaviour in the  $\beta$  phase for each compound is shown by log-log plots. For PAMC a deviation in the law is observed at  $T_{c2}$ , the start of the  $\gamma$  phase.

$\Delta n^\epsilon(T) \simeq 0.015 \times 10^{-3} T$ . At  $T_{c5}$  the amplitude disappears and is replaced by the  $\text{MnCl}_6$  octahedra rotation mechanism just as in the  $\gamma$  phase for EAMC. This produces a large negative change of 5% in  $\Delta n$  at  $T_{c5}$ ; in addition, a thermal hysteresis of 2 K was measured.

In the low-temperature  $\gamma$ (EAMC) and  $\zeta$ (PAMC) phases the optical anisotropy does not change very much but shows a very broad local minimum, approximately centred around 90 and 70 K, respectively. The well-known two-dimensional antiferromagnetic ordering (Kojima, Ban & Tsujikawa, 1978) in the  $\mathbf{ab}$  plane may be responsible for this behaviour. Preliminary studies, concentrating on the range  $T \leq 100$  K, indicate a slight anomaly in the birefringence around 39 K, possibly a contribution from three-dimensional ordering giving rise to an in-plane weak ferromagnetic moment at 39.2 K (Groenendijk, van Duyneveldt & Willet, 1979).

A comprehensive survey of the transition temperatures for both compounds is found in Table 1 along with a brief description for  $\Delta n(T)$  in each phase.

### The symmetry of $\epsilon$ -PAMC

The phase of PAMC existing between  $T_{c4}$  and  $T_{c5}$  is called the  $\epsilon$  phase. The delimiting phase transitions are quite different in character and that at  $T_{c5}$  is much more pronounced than that at  $T_{c4}$  from the point of view of enthalpy (Depmeier, Felsche & Wildermuth, 1977) as well as from that of birefringence (Fig. 1). The diffraction aspect of the  $\epsilon$  phase differs from those of the two phases above and below by the appearance of extra reflexions (satellites) which cause a tripling of the  $b$  axis. This fact has already been mentioned in the 1977 paper of Depmeier, Felsche & Wildermuth, but at that time a better understanding of this superstructure was not possible because the X-ray and cooling equipment used restricted the observable range of the reciprocal space. It was, therefore, only after performing a neutron experiment (Depmeier & Mason, 1982) and also after becoming more familiar with the de Wolff approach of supersymmetry in modulated structures (de Wolff, 1977) that it was possible to get some insight into the symmetry relations of this phase.

The method of analysing the satellite reflexions has already been used for the description of the incommensurately modulated  $\gamma$  phase of PAMC (Depmeier, 1981), where also a brief introduction to this method has been given. The method has been developed by de Wolff (1974, 1977), Janner & Janssen (1977), Janner, Janssen & de Wolff (1979) and Janssen & Janner (1979), to which the reader is referred for more information about this subject.

Fig. 3 shows schematically the distribution of main and satellite reflexions in the reciprocal space of

$\epsilon$ -PAMC. The main reflexions can be indexed using the following lattice parameters (at  $T = 136.5$  K):  $a = 7.445$  (2),  $b = 7.148$  (2),  $c = 25.483$  (7) Å and they obey the non-extinction rules for the space group  $Abma$  ( $hkl: k + l = 2n; 0kl: k = 2n; hk0: h = 2n$ ).

The satellites triple the  $b$  axis and they appear generally around existing main reflexions; only in the  $0kl$  reciprocal layer are they exclusively around extinct main reflexions. With the satellites included, the indexing can be achieved in two different ways. The first one is based on the supercell, *i.e.* with lattice dimensions  $a = 7.445$  (2),  $b' = 21.445$  (8),  $c = 25.483$  (7) Å. For this indexing a three-placed symbol  $hk'l$  can be used and one observes that by the formation of the superstructure the  $A$  centring is destroyed. The second one uses the lattice parameters of the subcell and indices  $hklm$  are used.  $m$  is the order of the satellites ( $\pm 1$  is only observable) and  $k'$  of the first notation equals  $3k + m$  of the second one.

We notice that the main reflexions of the  $\epsilon$  phase form a pattern which is very similar to that of the  $\delta$  phase and that, to a first approximation, it is only the satellite reflexions which distinguish the two phases. Transformed into direct space this means that the structure of  $\epsilon$  PAMC is a distorted version of the  $\delta$  phase. Using the picture of a distortion wave which alters the  $\delta$  phase, one can say that the modulation vector of that wave  $\mathbf{q}^*$  is parallel to  $\mathbf{b}^*$  and has a value

of  $1/3$ . No deviation from this rational number has been measured and we, therefore, call this phase a commensurate superstructure, following de Wolff (1974), or a locked-in phase, because the modulation vector does not (as far as we know) change with temperature.

The supersymmetry approach is not restricted to incommensurately modulated structures and we, therefore, are allowed to apply it to  $\epsilon$  PAMC, thus regarding this structure as one-dimensionally modulated (but with a fixed, locked-in modulation vector).

The diffraction pattern of  $\epsilon$  PAMC is invariant under the following point-group operations:

$$m_x = \begin{pmatrix} \bar{1} & & & \\ & 1 & & \\ & & 1 & \\ & & & 1 \end{pmatrix} \quad m_y = \begin{pmatrix} 1 & & & \\ & \bar{1} & & \\ & & 1 & \\ & & & \bar{1} \end{pmatrix} \quad m_z = \begin{pmatrix} 1 & & & \\ & 1 & & \\ & & \bar{1} & \\ & & & 1 \end{pmatrix}.$$

The diagonal matrices refer to indices  $hklm$  and the Laue group is  $\frac{2'}{m} \frac{2}{m'} \frac{2'}{m}$ , where a prime indicates a change in sign of the fourth index.

The components of  $\mathbf{q}^* = \alpha\mathbf{a}^* + \beta\mathbf{b}^* + \gamma\mathbf{c}^*$  are  $\alpha = 0$ ,  $\beta = 1/3$ ,  $\gamma = 0$ , hence, according to Janner, Janssen & de Wolff (1979),  $\sigma = (0, \beta, 0)$  with  $\beta = 1/3$ . A basis in  $R_4^*$  is, therefore,  $\mathbf{a}^*$ ,  $\mathbf{b}^*$ ,  $\mathbf{c}^*$ ,  $\mathbf{q}^* + \mathbf{e}^*$  ( $= \beta\mathbf{b}^* + \mathbf{e}^*$ ). Reciprocal to that we find the basis in  $R_4$ :  $\mathbf{a}$ ,  $\mathbf{b} - \beta\mathbf{e}$ ,  $\mathbf{c}$ ,  $\mathbf{e}$ , with  $\mathbf{e}$  being the basic vector in the fourth direction. Because of the validity of  $k + l$  even this is an  $A$ -centred basis.

For  $\sigma = (0, \beta, 0)$  and the condition  $k + l = 2n$  we find the Bravais group  $P_{111}^{Ammm}$ , which is No. 15 in the tables of de Wolff, Janssen & Janner (1981). If we assume that the basic space group is centrosymmetric and use the reflection conditions found,  $hklm: k + l = \text{even} \rightarrow$

$$A; 0klm: k + m = \text{even} \rightarrow \begin{pmatrix} b \\ s \end{pmatrix} \begin{pmatrix} c \\ s \end{pmatrix}; hk0m: h = \text{even} \rightarrow \begin{pmatrix} a \\ 1 \end{pmatrix},$$

we find four possible superspace groups [after applying

a transformation  $\begin{pmatrix} 100 \\ 001 \\ 0\bar{1}0 \end{pmatrix}$  to have the modulation in the

$b$  direction]:

$$P_{111}^{Abma}, P_{s11}^{Abma}, P_{s1s}^{Abma}, P_{11s}^{Abma}.$$

We use systematic extinctions to make a decision: Groups 3 and 4 demand that reflections  $hk0m$  are only present for  $h + m$  even. Because of the very manifest presence of first-order satellites around main reflexions with  $h = 2n$ ,  $k = 2n$  in this layer we can rule these superspace groups out. The second group  $P_{s11}^{Abma}$  demands a non-extinction rule  $0klm: k + m = 2n$ . This is exactly what we find (Fig. 3). Of course, we cannot exclude the presence of very weak satellites which

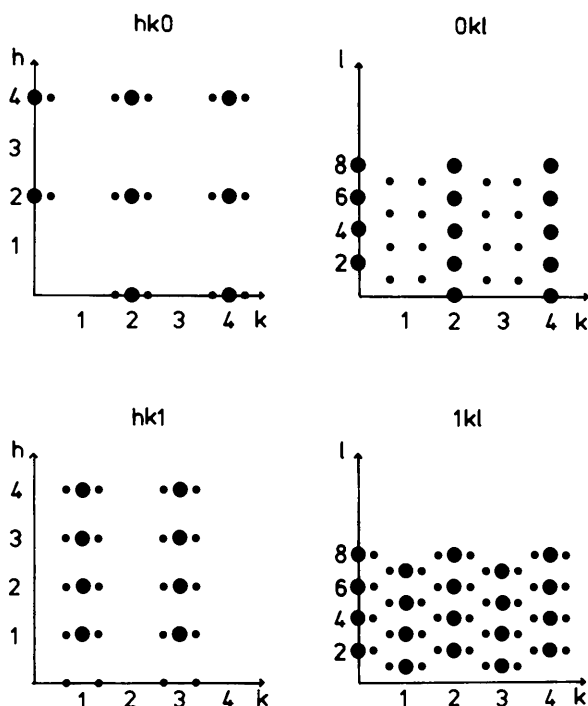


Fig. 3. Schematic drawing of main reflexions (large circles) and satellite reflexions (smaller circles) in the  $hk0$ ,  $hk1$ ,  $0kl$  and  $1kl$  reciprocal planes of PAMC. Indices refer to the subcell.

disobey this rule but to a very good approximation we can conclude that this group (or one of its subgroups) describes the symmetry of  $\varepsilon$ -Pamc. Another notation, proposed in the above-mentioned tables uses the numbering and this would be 64c.15.2 for this (3 + 1)-dimensional superspace group. Let us mention that this group is identical with  $P_{s11}^{Acen}$  and the corresponding non-extinction rules are, of course, fulfilled:  $hklm$ :  $k + l = 2n$ ;  $Oklm$ :  $l + m = 2n$ ;  $hkOm$ :  $h + k = 2n$  ( $h, k = 2n$ ). The non-extinction rule  $Oklm$ :  $k + m = 2n$  would also allow for second-order satellites around non-extinct main reflexions. They have, however, not been observed.

The generating symmetry operations for  $P_{s11}^{Abma}$  are:

$$m_x: (x, y, z, t) \rightarrow (\frac{1}{2} - x, \frac{1}{2} + y, z, t + \frac{1}{2})$$

$$m_y: (x, y, z, t) \rightarrow (x, \bar{y}, z, -t)$$

$$m_z: (x, y, z, t) \rightarrow (\frac{1}{2} + x, y, \frac{1}{2} - z, t)$$

with  $t$  being the coordinate in the fourth (modulating) direction of the superspace  $x\mathbf{a} + y\mathbf{b} + z\mathbf{c} + t\mathbf{e}$ .

We can get a picture of the structure of  $\varepsilon$ -PAMC as a distorted version of that of  $\delta$ -PAMC by applying the symmetry operations of  $P_{s11}^{Abma}$  to the structure of  $\delta$ -PAMC (a description of this basic structure may be

found in Depmeier, 1981). Owing to the  $\begin{pmatrix} b \\ s \end{pmatrix}_x$  and  $\begin{pmatrix} c \\ s \end{pmatrix}_x$

operations (both at  $x = 0.25$ ), atoms related by these operations have a phase shift of  $\pi$ . If we assume a symmetric distortion wave, say a sinusoidal one, then every third mirror plane of space group  $Abma$  in the  $y$

direction is retained. These are also the loci of the  $\begin{pmatrix} m \\ \bar{1} \end{pmatrix}_y$

operations and since  $\mathbf{q}^* = 1/3$  is rational, these mirror planes are part of a three-dimensional space group, which then becomes  $Pbma$ . Because of the non-space-group extinctions this group was difficult to establish unambiguously from the superstructure pattern with  $hk'l$ . This is also the space group in which the structure of  $\varepsilon$ -PAMC should be refined. It should be mentioned, however, that the superspace group  $P_{s11}^{Abma}$  tells much more about the symmetry relations in the distorted structure than does the three-dimensional space group  $Pbma$ .

We note that the satellites in the  $Oklm$  plane are much more pronounced than in the  $hkOm$  plane. This is similar to  $\gamma$ -PAMC (Depmeier, 1981) and gives us the idea that the amplitude of the distortion wave is parallel to the  $c$  direction and only an additional longitudinal component leads to the weak satellites observed in the  $hkOm$  plane.

The authors are very much indebted to Professor de Wolff for critically reading the paper and for comments.

## References

- DEPMEIER, W. (1976). *Acta Cryst.* B32, 303–305.  
 DEPMEIER, W. (1977). *Acta Cryst.* B33, 3713–3718.  
 DEPMEIER, W. (1981). *Acta Cryst.* B37, 330–339.  
 DEPMEIER, W., FELSCHE, J. & WILDERMUTH, G. (1977). *J. Solid State Chem.* 21, 57–65.  
 DEPMEIER, W. & HEGER, G. (1978). *Acta Cryst.* B34, 1698–1700.  
 DEPMEIER, W. & MASON, S. (1978). *Acta Cryst.* B34, 920–922.  
 DEPMEIER, W. & MASON, S. (1982). In preparation.  
 EGERT, G., JAHN, I. R. & RENZ, D. (1971). *Solid State Commun.* 9, 775–778.  
 GROENENDIJK, H. A., VAN DUYNVELDT, A. J. & WILLET, R. D. (1979). *Physica (Utrecht)*, 98B, 53–59.  
 JANNER, A. & JANSSEN, T. (1977). *Phys. Rev. B*, 15, 643–658.  
 JANNER, A., JANSSEN, T. & DE WOLFF, P. M. (1979). In *Modulated Structures – 1979, AIP Conf. Proc.* No. 53, edited by J. M. COWLEY, J. B. COHEN, M. B. SALAMON & B. J. WUENSCH, pp. 81–83. New York: American Institute of Physics.  
 JANSSEN, T. & JANNER, A. (1979). Proceedings of the 4th European Meeting on Ferroelectricity, Portoroz.  
 KNORR, K., JAHN, I. R. & HEGER, G. (1974). *Solid State Commun.* 15, 231–238.  
 KOJIMA, N., BAN, T. & TSUJIKAWA, I. (1978). *J. Phys. Soc. Jpn*, 44, 919–922.  
 PETERSON, E. R. & WILLET, R. D. (1972). *J. Chem. Phys.* 56, 1879–1882.  
 WOLFF, P. M. DE (1974). *Acta Cryst.* A30, 777–785.  
 WOLFF, P. M. DE (1977). *Acta Cryst.* A33, 493–497.  
 WOLFF, P. M. DE, JANSSEN, T. & JANNER, A. (1981). *Acta Cryst.* A37, 625–636.